The populations of planetary nebulae in the direction of the Galactic bulge. Chemical abundances and Wolf-Rayet central stars

S. K. Górny, Grazyna Stasinska, A. V. Escudero, R. D. D. Costa

A&A 427, 231–244 (2004)
DOI: 10.1051/0004-6361:20047064

Astronomy & Astrophysics

The populations of planetary nebulae in the direction of the Galactic bulge⋆,⋆⋆

Chemical abundances and Wolf-Rayet central stars

S. K. Górny[1], G. Stasińska[2], A. V. Escudero[3], and R. D. D. Costa[3]

[1] Copernicus Astronomical center, Rabiańska 8, 87-100 Toruń, Poland
e-mail: skg@ncac.torun.pl
[2] LUTH, Observatoire de Meudon, 5 place Jules Janssen, 92195 Meudon Cedex, France
e-mail: grazyna.stasinska@obspm.fr
[3] Departamento de Astronomia, Instituto de Astronomia, Geofísica e Ciências Atmosféricas da USP, Rua do Matão 1226, 05508-090, São Paulo, Brazil

Received 13 January 2004 / Accepted 13 July 2004

Abstract. We have observed 44 planetary nebulae (PNe) in the direction of the Galactic bulge, and merged our data with published ones. We have distinguished, in the merged sample of 164 PNe, those PNe most likely to prtain physically to the Galactic bulge and those most likely to belong to the Galactic disk. We have determined the chemical composition of all the 164 objects in a coherent way. We looked for stellar emission features and discovered 14 new [WR] stars and 15 new weak emission line central stars.
The analyzed data led us to the following conclusions: (1) the spectral type distribution of [WR] stars is very different in the bulge and in the disk of the Galaxy. However, the observed distributions are strongly dependent on selection effects. (2) The proportion of [WR] PNe is significantly larger in the bulge than in the disk. (3) The oxygen abundances in [WR] stars do no appear to be significantly affected by nucleosynthesis and mixing in the progenitors. (4) The O/H gradient of the Galactic disk PNe population flattens in the most internal parts of the Galaxy. (5) The median oxygen abundance in the bulge PN population is larger by 0.2 dex than in the disk population seen in the direction of the bulge. (6) Bulge PNe with smaller O/H tend to have smaller radial velocities. (7) The oxygen abundance distribution of bulge PNe is similar in shape to that of the metallicity distribution of bulge giants, but significantly narrower. (8) The location of SB 32 (PN G 349.7-09.1) in the ($V_{\rm lsr}$, $l_{\rm II}$) diagram and its low oxygen abundance argues that it probably belongs to the halo population.

Key words. stars: Wolf-Rayet – ISM: planetary nebulae: general – Galaxy: bulge – Galaxy: abundances

1. Introduction

Planetary nebulae (PNe) are indicators of the chemical composition of the interstellar matter out of which the progenitors stars were born (mainly through the abundances of elements such as O, Ne, S). They are also indicators of the nucleosynthesis and mixing processes occurring in their central stars (mostly through the abundances of He, C, N).

Among planetary nebulae, those with central stars of Wolf-Rayet type have received considerable attention recently (e.g. Tylenda et al. 1993; Górny & Stasińska 1995; Peña et al. 2001; Blöcker et al. 2001; De Marco 2003; Acker & Neiner 2003). Planetary nebulae with Wolf-Rayet central stars ([WR] PNe) are believed to represent around 6–10% of the total population of planetary nebulae (Górny & Stasińska 1995; Tylenda 1996). Until recently, their mechanism of production was not well understood: how to obtain a PN nucleus whose atmosphere is almost completely devoid of hydrogen and essentially composed of helium and carbon? The late-helium flash scenario of Iben et al. (1983) could possibly account for only a minority of [WR] PNe, primarily those with an old nebular envelope surrounding a star of late [WC] type. Acker et al. (1996) and Górny & Tylenda (2000) have shown that the majority of [WR] PNe seem to draw an evolutionary sequence from late-type to early-type [WC] types. Recently, Herwig (2001) and Blöcker et al. (2001) showed that overshoot applied to models of stars in the AGB phase was able to produce abundances similar to those observed in [WR] stars, and that a final thermal pulse occurring on the AGB was able to produce [WR] PNe with young kinematic ages. However, De Marco & Soker (2002) make the point that the double dust chemistry in [WR] PNe revealed by ISO spectra requires a different

⋆ Based on observations made at the South African Astronomical Observatory.

⋆⋆ Tables 1–3 are only available in electronic form at the CDS via anonymous ftp to cdsarc.u-strasbg.fr (130.79.128.5) or via http://cdsweb.u-strasbg.fr/cgi-bin/qcat?J/A+A/427/231

explanation and propose a scenario where a low-mass star or planet spirals into the AGB star, enhancing the mass-loss rate and introducing extra mixing.

It is not clear yet whether [WR] PNe are produced only by a certain subclass of intermediate mass stars. Neither the morphology, nor the chemical composition, nor the Galactic distribution or kinematics of [WR] PNe seem to differ statistically from those of non-[WR] PNe (Górny & Stasińska 1995; Górny 2001). However, this statement needs to be reexamined using a better defined control sample of non-[WR] PNe.

A coherent analysis of a large sample of planetary nebulae in the direction of Galactic bulge offers the possibility of a more detailed comparison. One of the advantages of planetary nebulae in the direction of the galactic bulge is that their distances are known (to within about 10% at least for the majority of them). However, the population of planetary nebulae in the Galactic bulge is probably not the same as that of the Galactic disk, since the stellar population in the bulge is 10 Gyr old (Zoccali et al. 2003), while in the disk the stellar ages span the entire range from 10 Gyr to virtually zero (Chiappini et al. 2001). Therefore, it is also interesting to investigate whether the global properties of [WR] PNe in the Galactic bulge are different from those of disk [WR] PNe. In this respect, it is remarkable that in the Magellanic Clouds, the spectral types of [WR] PNe central stars lie between [WC4] and [WC8] (Peña et al. 1997) (except the nucleus of N66, which until recently was the only known [WN] type star until another case was found in our Galaxy by Parker & Morgan 2003) while the [WR] PNe known in the Galaxy are either of very late ([WC8] – [WC11]) or very early ([WC2] – [WC4]) types (Górny 2001; Acker & Neiner 2003), clearly avoiding the middle types for some unknown reason. This suggests that the WR phenomenon is dependent on the charateristics of the stellar population giving rise to the observed PNe. For the Galactic bulge, it has also been proposed that [WR] stars are mostly of intermediate spectral types (Górny 2001), although Acker & Neiner (2003) do not confirm such a view. However all these inferences are based on small samples.

In this paper, we first enlarge the sample of [WR] PNe towards the Galactic bulge, by presenting a new set of observations. We combine our observations with those of previous data sets which also allow us to detect the possible presence of stellar emission lines and to determine which of these PNe harbour a [WR] type central star (or weak emission line star (WELS) possibly related to [WR] stars, see e.g. Tylenda et al. 1993; Peña et al. 2001). The samples are described in Sect. 2, and rearranged into one sample of PNe pertaining physically to the Galactic bulge and another sample of PNe seen in the direction of the Galactic bulge but pertaining to the Galactic disk. In Sect. 3, we determine the chemical composition of all the PNe in the combined sample and discuss the accuracy of the derived abundances. In Sect. 4, we show the results of our search of [WR] stars and WELS in the entire sample. We define the spectral types of the newly discovered [WR] stars, and comment on the statistics of the [WC] types as well as on the physical location of the [WR] PNe, including a discussion of the observational selection effects. In Sect. 5, we comment on the chemical composition of the PNe, by comparing several subsamples. Our main conclusions are summarized in Sect. 6.

2. Observational data

2.1. New observations and reduction procedure

The main aim of our observations was to detect new Wolf-Rayet central stars in the direction of the Galactic center (i.e. within, say, 20 degrees from the Galactic center in Galactic longitude and 15 degrees in Galactic latitude). The selection of PNe for observations was based on two criteria. First, we have dismissed all PNe for which there already existed spectral information on the central star, i.e. the spectral type was known or the stellar continuum had been observed but no emission lines were seen (Tylenda et al. 1993, 1991). Next, we selected objects with IRAS mid-infrared colours similar to the colours of known [WR] PNe (see Górny et al. 2001). Therefore, obviously, this sample cannot be used to estimate the proportion of [WR] PNe among PNe in the Galactic bulge. For comparison purposes and to assess the quality of our spectra we also observed a few objects already known to have emission line central stars.

The spectra of the 44 objects of our observational sample were obtained in July 2000 with the 1.9-m telescope at the South African Astronomical Observatory. The spectral coverage was 3500–7000 Å with an average resolution of 1000. A slit width of 1.8 arcsec was selected, resulting in some loss of stellar light due to seeing conditions but allowing to avoid blending of important nebular lines. The typical integration time was 60 min (30 min if the central star was a known [WR] or WELS) with additional short time exposure to secure unsaturated spectra of the strongest nebular lines. The log of the observations is presented in Table 1. Two spectroscopic standard stars, Feige 110 and CD -32 9927, were also observed each night. A CuAr lamp exposure was taken before or after each PN spectrum for wavelength calibration purposes.

The reduction of the spectra was done with standard procedures of the MIDAS[1] (99NOV) longslit spectra package. These included bias subtraction, flat-field correction, atmospheric extinction correction, wavelength and flux calibration and extraction of the 1-dimensional spectra. The line fluxes were derived with the REWIA package (J. Borkowski; `http://www.ncac.torun.pl/~jubork`) adopting Gaussian profiles and performing multi-Gaussian fits in case of blended lines.

2.2. A merged sample of PNe in the direction of the Galactic bulge

Published spectroscopic data on planetary nebulae towards the Galactic bulge are numerous (see Stasińska et al. 1998, for a compilation until 1997). However, the only data that allow us to check for the presence of emission lines in the central stars are those of Cuisinier et al. (2000) (30 objects),

[1] MIDAS is developed and maintained by the European Southern Observatory.

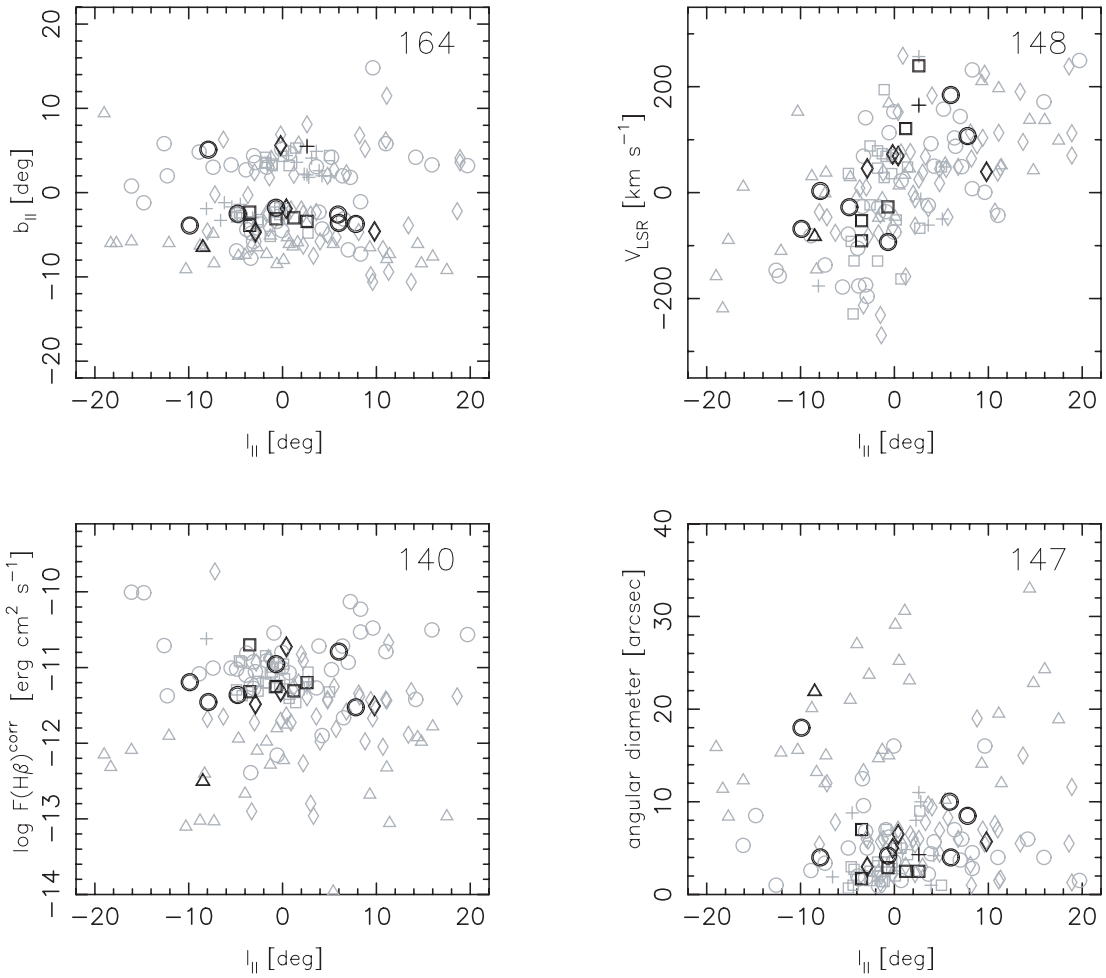

Fig. 1. Distribution in various diagrams of the PNe from our merged sample. *Top left*: b_{II} vs. l_{II}; *top right*: V_{lsr}, the radial velocities corrected for solar motion vs. l_{II}; *bottom left*: total nebular flux in Hβ corrected for reddening vs. l_{II}; *bottom right*: angular diameters as a function of l_{II}. The number on the top right of each panel gives the total number of objects represented in the plot. Objects pertaining to different samples are marked by different symbols: G: circles, C: squares, B: triangles, K: plus signs, E: diamonds. (See Sect. 2.2 for detailed definitions.) Symbols for [WR] PNe are thicker than for the rest of PNe.

Escudero & Costa (2001) (45 objects) and Escudero et al. (2004) (57 objects). We thus merged these three samples with the one described in Sect. 2.1, obtaining a total of 164 objects composing what we will refer to as the merged sample. In the case of duplicate spectra, we kept for further analysis the ones described in Sect. 2.1.

Figure 1 shows the distribution in various diagrams of the PNe from our merged sample. Each of the set of observations is marked by a different symbol: circles are for subset G (the set of observations described in Sect. 2.1), squares are for subset C (the sample of Cuisinier et al. 2000), triangles are for subset B (the objects from the list of Beaulieu et al. 1999 observed by Escudero & Costa 2001), plus signs for subset K (the objects from the list of Kohoutek 1994 observed by Escudero & Costa 2001) and diamonds for subset E (the objects observed by Escudero et al. 2004). [WR] PNe are marked by thicker symbols. The top left panel shows the Galactic latitude and longitude, b_{II} and l_{II}. The top right panel shows V_{lsr}, the radial velocities corrected for solar motion as a function of l_{II} (the radial velocities have been taken from Durand et al. 1998 and have been corrected from solar motion using the formulae given in Beaulieu et al. 2000). The bottom left panel shows the total extinction corrected nebular flux in Hβ[2] as a function of l_{II}. The bottom right panel shows the angular diameters as a function of l_{II}. A clear segregation of the various subsamples is seen. This is due to the various selection criteria used to define each sample. The sample of Cuisinier et al. (2000) is part of the list of PNe from Stasińska & Tylenda (1994) that lie within 10 degrees of the Galactic center, have radio fluxes and diameters measured with the VLA, with angular diameters smaller than 15 arcsec and radio fluxes at 6 cm between 10 and 100 mJy. The PNe from samples G and B extend over larger zones in l_{II} and b_{II}. But, while the objects from sample G are rather

[2] The Hβ fluxes for most of objects come from Acker et al. (1992) and have been corrected for interstellar extinction as determined from the ratio of the radio to Hβ fluxes if good quality radio flux measurements are available (references as in Stasińska et al. 1992). Otherwise the extinction has been derived from the Hβ/Hα ratio using values from Tylenda et al. (1994). For objects from the list of Beaulieu et al. (1999) we have calculated the Hβ fluxes from Hα fluxes given in this paper using the Hβ/Hα ratios from our spectra to calculate the extinction.

luminous, the objects from sample B are newly discovered PNe that are rather faint and have larger angular diameters. The objects from sample E are found in a more extended zone than the objects from sample C and are of intermediate luminosity. Since these different observational sets obey to different selection criteria, none of them can be considered to represent the population of the Galactic bulge and it is no surprise that each one may have different mean properties (as already noted by Escudero & Costa 2001). By merging these data sets, we are getting a more complete view of the PN populations in the direction of the Galactic bulge, although, unfortunately, none of the samples we consider is complete in any sense.

We can divide our merged sample of PNe into two distinct populations. The first one, hereafter referred to as *b*, is composed of objects lying within 10 degrees of the Galactic center, having angular diameters smaller than 20 arcsec and radio fluxes at 6 cm smaller than 100 mJy. About 95% of these objects are likely physically related to the Galactic bulge as shown by Stasińska et al. (1991). The second subsample, hereafter referred to as *d*, contains the remaining objects and most of them should be related to the Galactic disk population.

Note that this distinction between "bulge" and "disk" populations does not use the radial velocities of the nebulae. However, as already noted by Zijlstra et al. (1997), PNe thought to be physically related to the Galactic bulge exhibit a large range of radial velocities, between -250 km s^{-1} and $+250$ km s^{-1}. The distinction in kinematic properties between our subsamples *b* and *d* of PNe in the direction of the Galactic bulge is clearly seen by comparing Figs. 12 and 13 (to be fully described later), which repeat the ($V_{\rm lsr}$, $l_{\rm II}$) diagram for samples *b* and *d* respectively. Objects from sample *d* that are found at a Galactic longitude close to zero have a radial velocity close to zero, compatible with rotation in circular orbit in the Galactic disk.

3. Analysis of nebular emission lines

The chemical composition of the newly observed planetary nebulae was derived as described below. We also rederived the abundances of the PNe with published line intensities using the same methods in order to obtain a reasonably homogeneous set of abundances.

3.1. Reddening correction

The measured line intensities of the newly observed sample have first been corrected for interstellar extinction using the extinction law of Seaton (1979) and forcing the observed Hα/Hβ ratio to the theoretical recombination value. However, with such a procedure, the reddening-corrected Hδ/Hβ and Hγ/Hβ ratios were often significantly different than theoretically expected. We attribute this to the E-W orientation of the slit and to the fact that the spectra were taken at different airmasses (reaching values of 2) which resulted in substantial loss of registered light at short wavelengths. It is important, for abundance determinations, to use intensities of [O III] λ4363 and [O II] λ3727 as reliable as possible. Therefore we have used the Hδ/Hβ and Hγ/Hβ ratios and have calculated the values of the additional correction that would bring them to the teoretical recombination values. This correction was then linearly propagated to the observed fluxes at all wavelengths shorter of 4681 Å(Hβ). The resulting line fluxes are presented in Table 2 on the scale of Hβ = 100. We also give line identification and laboratory wavelengths.

The same additional correction procedure has been applied to the objects from Escudero & Costa (2001) and Escudero et al. (2004) samples that originally also revealed some deviations from the theoretical Balmer decrement as discussed in Escudero et al. (2004).

3.2. Nebular abundance determinations

The abundances were derived with the classical empirical method. The electron densities were obtained from the [S II] λ6731/6717 ratio, the electron temperatures from the [O III] λ4363/5007 and [N II] λ5755/6584 ratios. The ionic abundances and elemental abundances were then derived using the code ABELION as in Peña et al. (2001). The only difference is that here we used the collision strengths of Keenan et al. (1996) for [S II] lines. Those objects for which the electron temperature could be determined neither from [O III] λ4363/5007 nor from [N II] λ5755/6584 were discarded from abundance determinations. This concerns only 5 objects among 164 (4 in sample *b*, one in sample *d*). The temperature derived from [N II] was used for ions of low ionisation potential, that from [O III] λ4363/5007 for ions of high ionization potential. In general, the temperatures from [O III] λ4363/5007 and [N II] λ5755/6584 are similar, but often not identical within their error bars as shown in Fig. 2. If the temperature from [N II] was very uncertain, we rather used the temperature from [O III] λ4363/5007 for all the ions. We have adopted for the abundance of O^+ the mean of the abundances derived from the [O II] λ3727 and the [O II] λ7320, 7330 line, when available. A discussion of the comparison between both abundances can be found in Escudero et al. (2004). Table 3 lists the resulting plasma diagnostics and abundances for all the objects of the merged sample. Column 1 gives the PNG number; Col. 2 gives the usual name of the PN; Col. 3 indicates the observational subsample (G, C, B, K or E). Column 4 indicates whether the object belongs to sample "*b*" as defined in Sect. 2.2. Column 6 gives the electron density deduced from [S II] λ6731/6717, Cols. 7 and 8 give the electron temperature deduced from [N II] λ5755/6584 and [O III] λ4363/5007 respectively. Columns 9 gives the He/H ratio, Cols. 10–13 give the N/H, O/H, Ne/H, S/H ratios, respectively, in units of 10^{-6}. Columns 14–18 give He^+/H^+, He^{++}/H^+, O^+/H^+ as derived from the 3727 line, O^+/H^+ as derived from the 7325 line, O^{++}/H^+. Column 19 gives the logarithmic extinction at Hβ derived from the spectra. In this table, there are three rows for each object, and a fourth row used to separate the objects. The first row gives the values of parameters computed from the nominal values of the observational data. The second and third row give the upper and lower limit respectively of these parameters as derived taking into account the observational error bars.

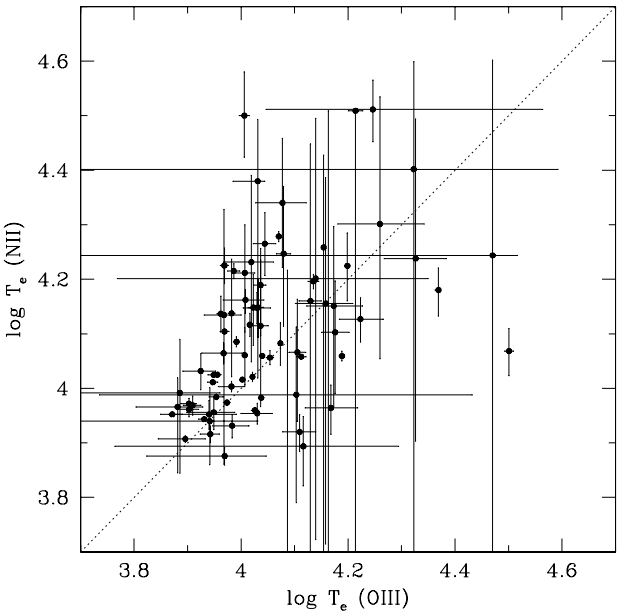

Fig. 2. The electron temperature derived from [O III] λ4363/5007 versus the electron temperature derived from [N II] λ5755/6584.

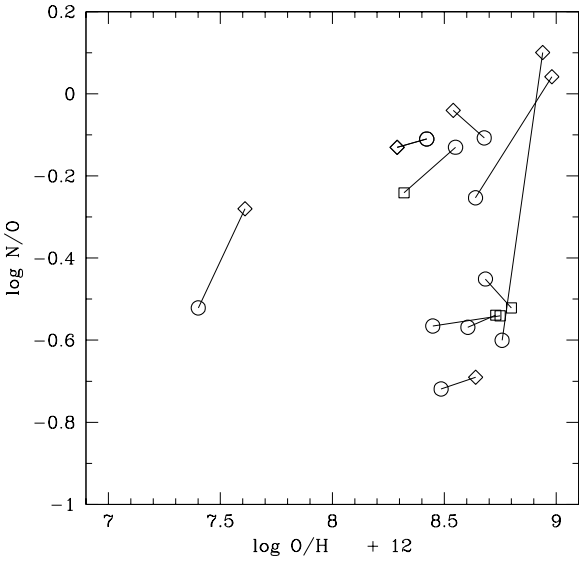

Fig. 3. The values of log N/O versus log O/H +12 for all the objects in common in the various data sets composing or merged sample. Symbols corresponding to the same object are linked by thin lines. The meaning of the symbols is the same as in Fig. 1.

Errors in the derived abundances result not only from observational errors (including the dereddening procedures), but also from uncertainties in the atomic data and the adequacy of the abundance derivation scheme. Comparing abundances derived by different authors for the same objects gives an idea of the uncertainty including all the sources of errors. This is shown in Fig. 3, where we plot the values of log N/O versus log O/H +12 for all the objects in common among several of the subsamples we considered. Values pertaining to the same object are linked by thin lines. The symbols are the same as in Fig. 1. From this figure, we conclude that global uncertainties in abundance ratios are typically of 0.2–0.3 dex for O/H but can be much larger in some cases for N/O. Apart from different determinations of the temperatures, the main source of uncertainty in the oxygen abundance is the estimation of O^+/H^+, especially in low excitation objects. The [O II] λ3727 line is severely affected by reddening, while the [O II] λ7320, 7330 line is intrinsically much weaker, more dependent on temperature and strongly affected by possible recombination. Both lines are sensitive to density, but in different ways. The N/O ratio is less affected by errors in the electron temperature than the O/H ratio. On the other hand, its derived value strongly depends on the value adopted for the O^+ abundance. Quite often, a difference in N/O between the determination by two authors traces back to a different estimate of the electron density, which has important consequences for very dense nebulae.

For helium, the expected errors in the abundances are much smaller, except in the case of PNe of very low excitation, where no correction can be made for the presence of neutral helium. However, even for high excitation nebulae, the errors are relatively large compared to expected object-to-object variations.

The lowest oxygen abundances found in our merged sample are as low as log O/H + 12 = 7.1–7.2. One may suspect that such low values are not real but result simply from an overestimated electron temperature (which, in general, is the main source of uncertainty in the oxygen abundance derivation). In Fig. 4, we plot the value of the electron temperature T_e, as derived from [O III] λ4363/5007, as a function of the computed value of log O/H + 12, together with the observational error bar on T_e and the error bars on log O/H resulting only from T_e. This figure shows that indeed, some of the lowest derived abundances are affected by large error bars, implying that the true abundances might be significantly higher than derived. However, there are four objects, for which log O/H + 12 is definitely smaller than 7.6. We are, of course, aware of the fact that recombination lines in planetary nebulae lead to larger values of the elemental abundances, sometimes by factors up to 10 (see e.g. Liu 2002 for a review). Here we adopt the view, as in all statistical studies on abundances so far, that the abundances derived from the forbidden lines are representative of the chemical composition in the bulk of the nebula.

4. [WR] PNe

4.1. Search for new [WR] PNe

We first searched our new spectra for the presence of emission line central stars. The distinction between [WR] stars and WELS is made as in Tylenda et al. (1993) on the basis of the strength and width of the C IV λ5805 doublet. This doublet is often seen as two separate components in WELS and is much weaker and narrower than in [WR]-type stars. It is the only stellar emission line seen in the spectra of WELS, among the lines used to classify [WR] stars. Note that the difference between [WR] stars and WELS is not always easy to make and one may suspect that better quality spectra could perhaps reveal additional spectral features especially for cooler stars.

We found 4 new [WR] stars and 8 new WELS in sample G, in addition to the 3 [WR] stars and 8 WELS already known to exist in this sample.

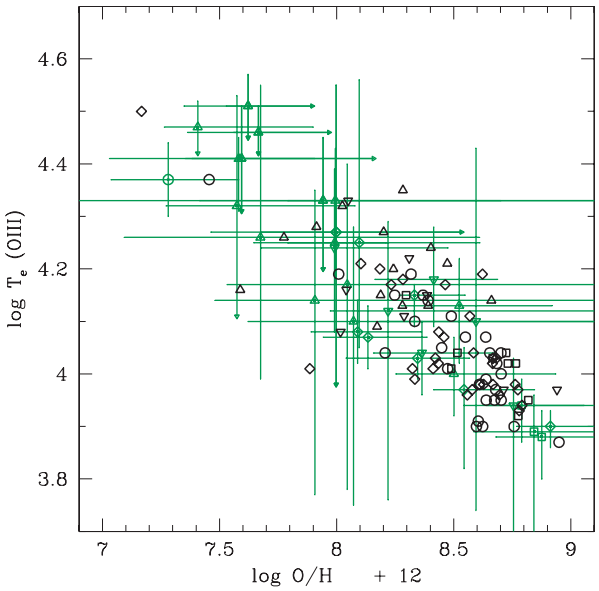

Fig. 4. The value of the electron temperature T_e as derived from [O III] λ4363/5007 as a function of the computed value of log O/H + 12. The observational error bar on T_e and the error bar on log O/H resulting from the error in T_e is shown (unless the error in log T_e is smaller than 0.1 and the error in log O/H smaller than 0.2, in which case the symbol is marked with a black heavy line). Arrows indicate that only an upper limit on T_e or a lower limit on O/H ca be obtained. The shape of the symbols has the same meaning as in Fig. 1.

We also examined the spectra of Escudero & Costa (2001) and Escudero et al. (2004). In the Escudero & Costa2001) subsample we found 2 [WR] stars and 3 WELS among 45 PNe. In the Escudero et al. (2004) sample we found 3 new [WR] stars and 4 new WELS in addition to the 1 known [WR] and 1 known WELS.

The observations by Cuisinier et al. (2000) are published only as a list of emission lines, among which lines of C III λ5695 and C IV λ5805 appear. These lines are in fact of stellar origin and we attribute them to [WR] stars. With these criteria, we find 5 new [WR] PNe in the sample of Cuisinier et al. (2000).

In total, including the [WR] and WELS already known, we find 18 [WR] and 24 WELS among 164 objects considered. The rate of occurence of [WR] PNe in the direction of the bulge is thus somewhat higher than that found by Tylenda et al. (1993) by examining 350 PNe spectra in the whole Galaxy. The ratio of WELS is much higher. This is likely due to two reasons. First, the spectra we examined are of substantially better quality than those examined by Tylenda et al. (1993), which came from a snapshot spectroscopic survey of the Galaxy. Second, our own observations were conducted on a sample specially designed to favor new discoveries of [WR] PNe, as explained in Sect. 2.1.

In the following of this paper, we will concentrate on [WR] PNe and their comparison with remaining PNe.

Table 4 presents all the PNe in the direction of the Galactic bulge whose nuclei were found to present emission lines. The [WR] stars and WELS discovered by us constitute "group 1". The [WR] stars and WELS that were already known to exist in the samples we analyzed constitute "group 2". There are also 15 [WR] PNe and 11 WELS reported in the literature to exist in the direction of the Galactic bulge but that do not belong to our "merged" sample[3]. They are also listed in Table 4 for completeness, under "group 3". For each of these groups, Col. 1 gives the PN G number; Col. 2 gives the usual name of the PN; Col. 3 indicates the observational subset (using the same convention as in Col. 3 of Table 3); Col. 4 indicates whether the object belongs to sample *b* as defined in Sect. 2.2; Col. 5 gives the *FWHM* of the C IV λ5805 or C III λ5695 line; Col. 6 gives the category of the star: W for [WR], w for WELS. For convenience, the same indications (i.e. W or w), are reported also in Col. 5 of Table 3.

Figure 5 presents the spectra of all the objects we identifed as [WR] PNe in samples G, B, K and E.

4.2. [WR] PNe spectral classification

The classification criteria we used followed the classical scheme (van der Hucht et al. 1981; Méndez & Niemela 1982; Hu & Bibo 1990) which is based solely on relative intensities of selected lines: C IV λ 5805, C III λ5695, C II λ5663, O VII λ5670, O VI λ5290 and O V λ5595. In addition, the presence of O VI λ3822 and C II λ7235 was also checked. The O VI λ3822 line is expected to be several times brighter than the basic C IV λ5805 line in early [WC] spectral types, therefore even if subject to large extinction it may be more easily detectable than the C IV λ5805 line. On the other hand C II λ7235 is expected to be the brightest line in the late [WC] types (Acker & Neiner 2003) and replaces the hardly detectable C II λ5663 line originally proposed by Hu & Bibo (1990).

Recently two refined classifications schemes have been proposed for Wolf-Rayet central stars of planetary nebulae based on quantitative criteria (Crowther et al. 1998; Acker & Neiner 2003). The first one imposes identical criteria of classification for massive population I WC stars and central stars of planetary nebulae but requires good quality spectra in order to derive reliable equivalent width measurements of stellar emission lines, especially if the nebular continuum is dominating. The second one is, in principle, better adapted to the CSPN specificity. Unfortunately, the primary criteria are not clearly defined. In addition, the ranges in line ratios defining the classes show strong discontinuities. Finally, the classification of early-types is not independent of the chemical composition. For all these reasons we decided to continue to use in this work the classical criteria. These criteria are more suited

[3] Recently, 2 additional [WR] PNe were discovered in the direction of the Galactic bulge (Parker & Morgan 2003) during a follow-up spectroscopic survey of 1000 new PNe candidates proposed from visual scans of AAO/UKST narrow-band Hα survey of the Milky Way (Parker et al. 1999, 2003). However, among 700 objects observed to date, only 7 new [WR] PNe were found (Parker & Morgan 2003). This very low detection rate possibly involves important selection effects and these new objects have to be considered separately in future works. *Note added in proof:* However, note also that 90% of these 1000 PN candidates do not yet have central star identified (Parker, priv. commun.).

Table 4. [WR] and WELS planetary nebulae in the direction of the Galactic bulge.

PN G	Name	Sample	Bulge	*FWHM*	*W*/*w*	type	spectra details or reference	Acker & Neiner (2003)
1	2	3	4	5	6	7	8	9
Group 1: [WR] PNe discovered in this work								
000.4+04.4	K 5-1	E	b	16.0	w	wels		
000.7+04.7	H 2-11	G[2]	b	18.0	w	wels		
000.9-02.0	Bl 3-13	E	b	7.8+7.4	w	wels		
001.2-03.0	H 1-47	C	b		W	[WC11]?	CIII present, CIV absent	(? – very late)
002.6-03.4	M 1-37	C	b		W	[WC11]?	CIII present, CIV absent	(? – very late)
002.6+05.5	K 5-3 [1]	K	b	28.2	W	[WC4]	CIV strong, OV > OVI, OVI 3822 present	([WO3])
003.6+03.1	M 2-14	G	b	21.8	w	wels		
005.9-02.6	MaC 1-10	G	b	37.4	W	[WC8]	CIV ≈ CIII	([WC7-8])
006.5-03.1	H 1-61	G	b	12.6+11.2	w	wels		
008.3-01.1	M 1-40	G		instr+instr	w	wels		
008.1-04.7	M 2-39	E	b	19.4	w	wels		
008.3-07.3	NGC 6644	G		6.0+6.8	w	wels		
009.6+14.8	NGC 6309	G		8.7+7.3	w	wels		
009.8-04.6	H 1-67	E		30.3	W	[WC2-3]	CIV present, OVI5290 ?, OVI3822 strong	([WO2]?)
009.6-10.6	M 3-33	E		7.6+7.8	w	wels		
013.7-10.6	Y-C 2-32	E		7.3+6.7	w	wels		
014.4-06.1	SB 19	B		15.3	w	wels		
343.9-05.8	SB 30	B		9.2	w	wels		
347.4+05.8	H 1-2	G		instr+instr	w	wels		
350.1-03.9	H 1-26	G		34.8	W	[WC4-5]	CIV ≫ CIII, OV > OVI & OV > CIII	([WO4])
351.5-06.5	SB 34	B		31.6	W	[WC2]	CIV present, OVI 3822 very strong, OVI 5290 ?, OVII 5670 ?	([WO2])
351.7-06.6	SB 35	B		instr+instr	w	wels		
352.1+05.1	M 2-8	G[2]	b	31.8	W	[WC2-3]	OVI5290 present, OVI3822 present	([WO3])
356.1+02.7	Th 3-13	G	b	21.5:	w	wels		
356.5-02.3	M 1-27	C	b		W	[WC11]?	CIII present, CIV absent	(? – very late)
356.5-03.9	H 1-39	C	b		W	[WC11]?	CIII present, CIV absent	(? – very late)
357.1-04.7	H 1-43	E	b	instr [3]	W	[WC11]	CIII present, CIV absent, CII ?	(? – very late)
359.8+05.6	M 2-12	E	b	instr [3]	W	[WC11]	CIII present, CIV absent, CII present	(? – very late)
359.3-01.8	M 3-44	G	b	instr [3]	W	[WC11]	CIII present, CIV absent, CII ?	(? – very late)
359.3-03.1	M 3-17	C	b		W	[WC11]?	CIII present, CIV absent	(? – very late)
Group 2: known [WR] PNe belonging to our "merged sample"								
000.4-01.9	M 2-20	E	b	28.0	W	[WC5-6]?	10*	[WC5-6]
002.6+08.1	H 1-11	E	b	instr+instr	w	wels		
004.2-04.3	H 1-60	G	b	instr+instr	w	wels		
006.4+02.0	M 1-31	G	b	25.3	w	wels		
006.0-03.6	M 2-31	G	b	41.8	W	[WC4-5]?	10*	[WC4]
007.8-03.7	M 2-34	G	b	no emission	W	[WC]	1	
007.0-06.8	VY 2-1	G	b	instr+instr	w	wels		
351.1+04.8	M 1-19	G		17.7	w	wels		
355.2-02.5	H 1-29	G	b	34.3	W	[WC4-5]?	10*	[WC4]
356.2-04.4	Cn 2-1	G	b	no emission	w	wels		
356.7-04.8	H 1-41	G	b	instr+instr	w	wels		
357.1+03.6	M 3-7	G	b	16.2	w	wels		
359.9-04.5	M 2-27	G	b	22.5	w	wels		
Group 3: known [WR] PNe not belonging to our "merged sample"								
001.5-06.7	SwSt 1				W	[WC10]	6*, 8*, 10*	[WC9]pec
002.4+05.8	NGC 6369				W	[WC4]	1, 3, 10*	[WO3]
002.0-06.2	M 2-33		b		w	wels	9	
002.2-09.4	Cn 1-5		b		W	[WC4]	1, 10*	[WO4]pec
002.0-13.4	IC 4776				w	wels	9	
003.1+02.9	Hb 4				W	[WC4]	8*, 10*	[WO3]
003.9-14.9	Hb 7				w	wels	9	
004.6+06.0	H 1-24		b		w	wels	9	
004.9+04.9	M 1-25		b		W	[WC6]	2, 10*	[WC5-6]
006.8+04.1	M 3-15		b		W	[WC5]	10*	[WC4]
007.8-04.4	H 1-65		b		w	wels	9	
009.4-05.0	NGC 6629 [4]				W	[WC5-6]	7	[WC4]?
010.8-01.8	NGC 6578 [4]				W	[WC4-6]	7	
011.9+04.2	M 1-32				W	[WC4]	10*	[WO4]pec
011.7-00.6	NGC 6567 [4]				W	[WC5-6]	7	
012.2+04.9	PM 1-188				W	[WC10]	6*, 5, 10*	[WC10]
012.5-09.8	M 1-62				w	wels	9	
014.3-05.5	V-V 3-6				w	wels	9	
016.4-01.9	M 1-46				w	wels	9	
017.9-04.8	M 3-30				W	[WC2-3]	10*	[WO2]
019.7-04.5	M 1-60				W	[WC4]	2	[WC4]
019.4-05.3	M 1-61				w	wels	9	
341.8+05.4	NGC 6153				w	wels	9	
352.9+11.4	K 2-16				W	[WC11]	1, 4, 8*, 10*	[WC11]
355.9-04.2	M 1-30		b		w	wels	9	
358.3-21.6	IC 1297				W	[WC3-4]	1, 10*	[WO3]

Notes: 1) K 5–3 = IRAS17276-2342 in Acker et al. (1996); 2) spectra of Escudero & Costa (2001) (sample E) were used to measure stellar emissions; 3) *FWHM* of C III λ5695; 4) objects classified as WELS in Peña et al. (2001).

References: 1) Tylenda et al. (1993); 2) Acker et al. (1996); 3) Koesterke & Hamann (1997); 4) Leuenhagen et al. (1996); 5) Leuenhagen & Hamann (1998); 6*) reclassified using data of Crowther et al. (1998); 7) Peña et al. (2001); 8*) reclassified using data of de Araújo et al. (2002); 9) Acker & Neiner (2003); 10*) reclassified using data of Acker & Neiner (2003).

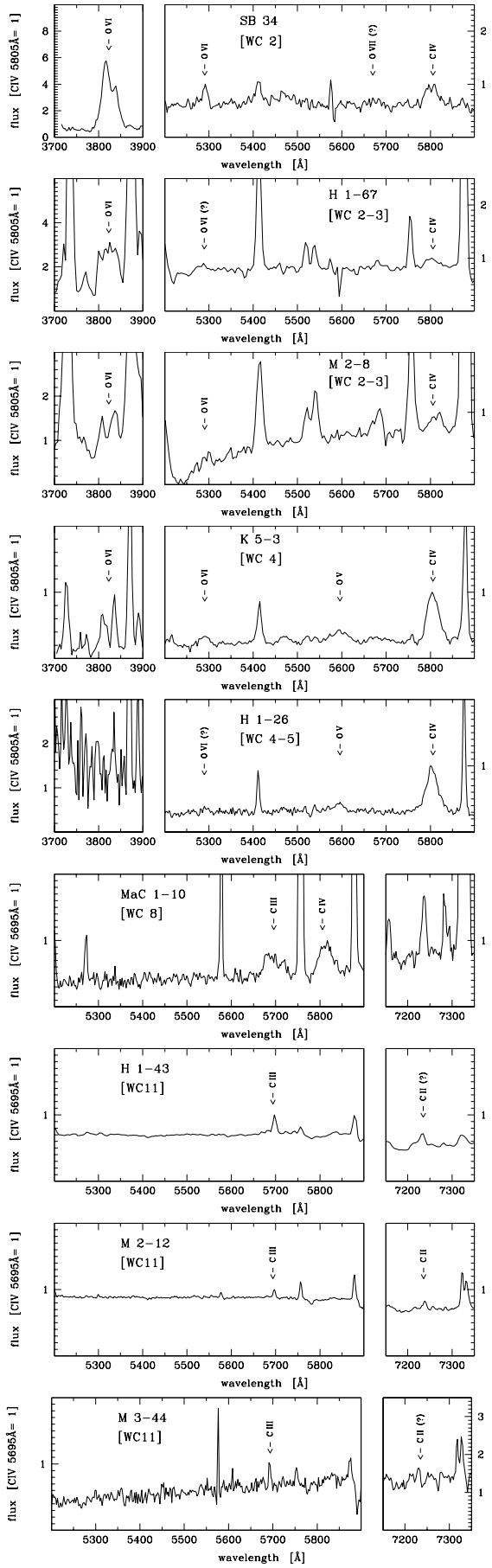

Fig. 5. Spectra of the newly discovered [WR] PN.

to the quality of our observations and can be directly compared to most of previous classification works.

The results of our spectral classification of [WR] stars are presented in Cols. 7 and 8 of Table 4. Column 7 gives the [WR] type. Column 8 describes the details of our spectra indicating this type or gives the references of the papers were the classification was published. For reference purposes, Col. 9 gives the spectral class assigned by Acker & Neiner (2003) to the [WR] PNe known at that time. We have tried to use the classification scheme of Acker & Neiner (2003) also to our newly discovered [WR] PNe. The results are given in the same column in parenthesis.

As can be seen from Table 4, a large proportion of the [WR] stars we discovered can be best described as late [WC11] type using the long-used, classical classification scheme adopted here. Their spectra look as expected for a very late WC type at a large distance. They are characterized by the presence of the narrow (*FWHM* < 5 Å) C III λ5695 line and the absence of the C IV λ5805 line. Therefore they fulfil one of the criteria to classify them as [WC11] (Hu & Bibo 1990). For some objects, especially the ones belonging to sample C, a classically definied [WC10] type cannot be excluded, since better spectra might reveal the presence of weak C IV lines. Interestingly, the C II λ7235 line was definitely seen in only one of the spectra we examined, while it was proposed that the [WC11] type should be dominated by both C III and C II lines (Hu & Bibo 1990). Again, this might be because the C II lines are too weak to be detected in our spectra therefore we regard this classification criteria as less important and imprecise.

Note that even the new classification schemes would require some clarification as far as the [WC11] class is concerned. In both papers (Crowther et al. 1998 and Acker & Neiner 2003), only one object, K 2–16, is classified as [WC11]. The defining criteria of the [WC11] class are obtained by extrapolation of the properties from adjacent classes and it is therefore not certain what intensity of C II lines should be expected. It must also be mentioned that K 2–16 has a rather unusual spectrum showing C IV λ5805 and O V λ5595 in absorption and surprisingly also some photospheric lines not expected to be present in [WR] stars (Crowther et al. 1998; de Araújo et al. 2002). It was proposed by Peña et al. (2001) that this object may have undergone a late helium-shell flash, so that it did not follow the common evolutionary path in which the [WR] phenomenon appears just after the AGB phase (see Górny & Tylenda 2000). This is supported by the distinct properties observed for K 2–16 in the infrared domain (Górny et al. 2001; Szczerba et al. 2001; Szczerba et al. 2003).

4.3. Statistics of [WR] types

Having determined which of the [WR] PNe are most likely physically linked to the bulge (see Sect. 2.2), we can compare the distributions of [WC] types in the bulge and in the disk.

Figure 6 shows the histograms of [WC] types for [WR] PNe pertaining to the bulge (top) and for [WR] PNe pertaining to the disk population (bottom). If we consider only objects from our "merged sample" (described in Sect. 2.2.) it is remarquable that

all the three [WR] PNe in sample "*d*" are of type earlier than [WC6] while there are only 5 such objects among 14 in sample "*b*". Since the statistics for our sample "*d*" are extremely low, we consider in the Fig. 6 all the known [WR] PNe by merging the ones from Table 4 with those collected in the litterature by Górny & Tylenda (2000). The top histogram concerns [WR] PNe of the Galactic bulge population, the bottom one shows all the known [WR] PNe pertaining to the entire Galactic disk. The litterature data add to our "merged sample" only 3 [WR] PNe in the bulge, but increases the disk sample from 3 to 46 (as most of the known [WR] PNe lie outside the direction of the galactic bulge). The difference between the bulge and disk histograms is highly significant.

First, we find a much larger proportion of [WR] stars later than [WC10] in the entire bulge sample (47%) than in the disk sample (17%). Second, the [WR] PNe in the direction of the Galactic bulge are underrepresented in spectral types [WC2] and [WC3] with respect to Galactic disk [WR] PNe. We have found only one such case (M 2–8) (i.e. 6%) in the Galactic bulge while there are 26% of objects in the disk sample. Note, finally, that the proportion of intermediate classes ([WC5] to [WC6]) is significantly larger in the bulge sample (22%) than in the disk sample (11%). We thus confirm the claims by Górny (2001) which were based on the analysis of much smaller samples.

It has been suggested (e.g. Górny & Tylenda 2000; Peña et al. 2001) that the [WC] sequence is an evolutionary sequence, with most of the late-type [WC] being surrounded by high density PNe and most of the early-type [WC] being surrounded by low density PNe. In Fig. 7, we show the nebular density deduced from [S II] λ6731/6717 as a function of the [WC] type for all the newly discovered [WR] PNe. The same trend is found as previously, well in line with the hypothesis that most [WR] PNe draw their evolution directly from the AGB.

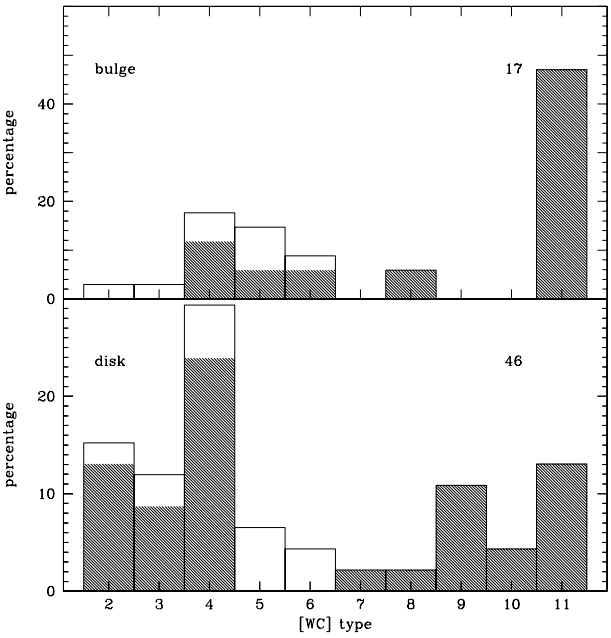

Fig. 6. The histograms of [WC] types for [WR] PNe in the Galactic bulge as defined in Sect. 2.2 (*top*) and in the Galactic disk (*bottom*) for all known [WR] PNe in the Galaxy including our newly discovered sources. The total number of objects used to construct each histogram is given in the upper right corner. The empty parts of the bars correspond to [WC 2–3], [WC 3–4] [WC 4–5], [WC 4–6] and [WC 5–6] types, distributed over two neighbouring bins.

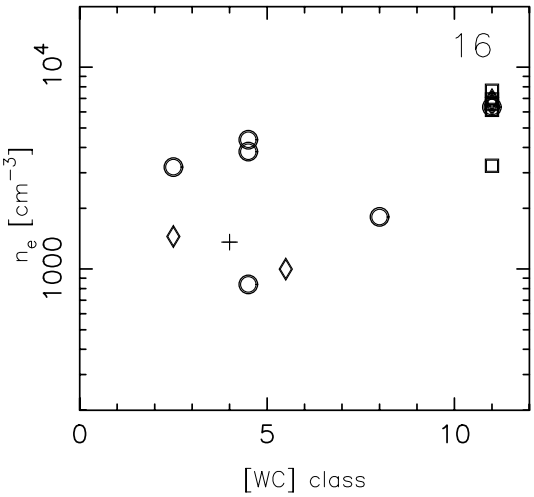

Fig. 7. The nebular density deduced from [S II] λ6731/6717 as a function of the [WC] type for all the newly discovered [WR] PNe. Objects pertaining to different samples are marked with the same symbols as in Fig. 1.

4.4. Selection effects

It may be surprising that most of the [WR] PNe we discovered are of late types, since one would expect the earliest [WC] types to be more easily detectable than the latest types, because the stellar features are both wider and stronger. However, before interpreting our findings in terms of stellar evolution or stellar masses, one should examine the selection effects more closely.

First of all, in the bulge, where the conditions of detection of PNe are difficult due to high extinction and crowding, there is a discrimination against detection of PNe with very hot central stars, because such nebulae are less luminous and more diffuse. This probably explains, at least in part, why the proportion of PNe with high effective temperatures is higher in the disk than in the bulge, as seen in Fig. 8 which compares the observed distribution of of He II Zanstra temperatures, $T_{\rm Zan}$(He II), in the bulge (upper panel) and in the disk (lower panel). To construct this figure, we have used the criteria described in Sect. 2.2 to divide the Strasbourg-ESO catalogue of Galactic PNe (Acker et al. 1992) into one subsample of 263 objects that most likely belong to the bulge, and one subsample of 878 objects which, for their vast majority, belong to the disk. We computed $T_{\rm Zan}$(He II) for all the PNe with central stars hot enough to ionise He^+ and for which the necessary data could be found in Acker et al. (1992) and Tylenda et al. (1994), obtaining values of He II Zanstra temperatures for 90 PNe in the bulge and 386 in the disk. The error bar on $T_{\rm Zan}$(He II) is typically of 0.05 in the log. The dashed bars in Fig. 8 stand for the objects present in our G, C or E subsamples. We see that, in the bulge, the number of PNe with sufficiently

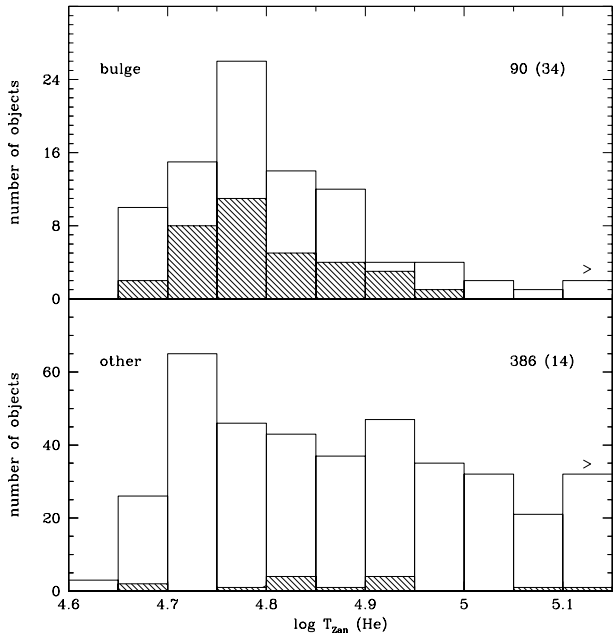

Fig. 8. The histogram of Zanstra He II temperature for the PNe catalogued in Acker et al. (1992) that pertain to the Galactic bulge (*upper panel*) and for the remaining PNe (*lower panel*). The number of objects used to construct the plot is given in the top right of each panel. The dashed bars stand for objects in common with our G, C or E samples and their number is given in parenthesis.

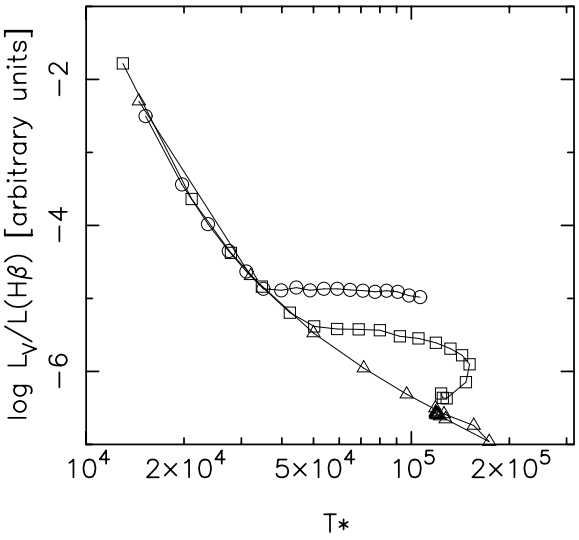

Fig. 9. The ratio $L_V/L(\mathrm{H}\beta)$ as a function of the star effective temperature, $T*$, for a series of simple models of expanding planetary nebulae around central stars of different masses (see text). Symbols are placed every 500 yr. Circles: $M_\star = 0.58\ M_\odot$; squares: $M_\star = 0.60\ M_\odot$; triangles: $M_\star = 0.62\ M_\odot$.

hot central stars (log T_{Zan}(He II) > 4.9) is very small, making the discovery of an early type [WC] star very unlikely. It is also interesting to note that the proportion of objects in the range 4.7 > log T_{Zan}(He II) > 4.85 (corresponding to the temperatures of intermediate [WC] types) is in fact similar in both groups of PNe: 21% (55/263) for the Galactic bulge objects and 18% (154/878) for the remaining PNe.

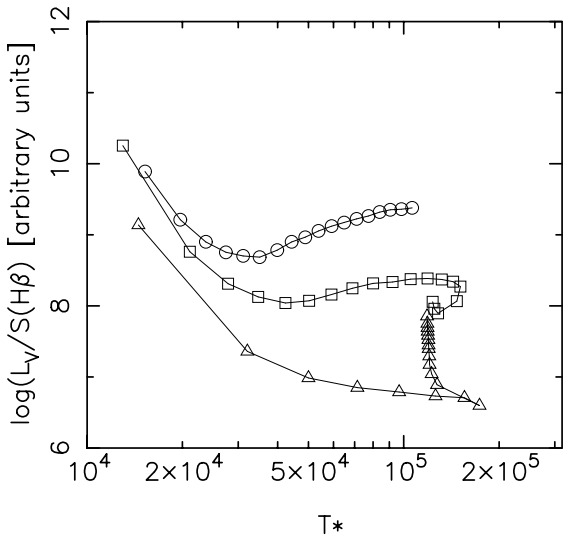

Fig. 10. The ratio $L_V/S(\mathrm{H}\beta)$ as a function of $T*$. Same models and same presenation as in Fig. 9.

Next, one must consider the condition of detection of the stellar emission lines.

PNe in the bulge have small angular dimensions, so that a large fraction of their total nebular flux is recorded in their spectra. Therefore the detection of [WR] PNe is possible only for objects in which the luminosity of the star in the V band (L_V) is sufficiently large with respect to the total nebular continuum emission (which is proportional to the luminosity in Hβ). For illustrative purposes, we show in Fig. 9 the ratio $L_V/L(\mathrm{H}\beta)$ as a function of the star effective temperature, $T*$, for a series of simple models of expanding planetary nebulae around central stars of different masses (the central stars evolve according to an interpolation of Blöcker (1995) evolutionary tracks, the nebulae are homogeneous with a total mass of 0.3 $M_\odot$, and the expansion velocity of the outer rim is taken to be 20 km s^{-1}). This corresponds to the extreme case where the entire nebula is covered by the region of the slit where the spectrum is extracted). This figure shows that the most favourable cases for detection of [WR] features in nebulae of small angular dimentions are those corresponding to the lowest stellar temperatures, i.e. to the latest spectral types, despite the fact that stellar emission lines are stronger in early-types.

On the contrary, many of the PNe known in the Galactic disk are relatively close-by, and have large angular dimensions, so only a small fraction of the nebular emission is recorded in the spectrograph slit. Then, a [WR] star will be preferentially detected in PNe with large $L_V/S(\mathrm{H}\beta)$ (where $S(\mathrm{H}\beta)$ is the nebular surface brightness in Hβ). Figure 10 shows this ratio as a function of $T*$ for the same models as Fig. 9. We see that, the conditions of detectability of [WR] features are more complicated. In the early phases of evolution, the $L_V/S(\mathrm{H}\beta)$ ratio is large, but this regime does not last long. At intermediate values of $T*$, the conditions of detectability of stellar features are less favourable. Finally, at high values of $T*$, the $L_V/S(\mathrm{H}\beta)$ ratio increases due to the expansion of the nebula, and the star becomes easier to observe, especially if the object is close-by.

Note that, especially for close-by nebulae with high temperature central stars, stellar features are much easier to detect for low than for high central star masses.

The distribution of [WR] stars among spectral classes is thus highly dependent on the selection effects just described. In addition, one must recall that the quality of the spectra used for the discovery and classification of [WR] PNe is very heterogeneous. For example, the quality of our new observations presented in Sect. 2.1, specially aimed at discovering new [WR] PNe is much higher than that of the survey on which was based the seminal paper by Tylenda et al. (1993). All this badly hampers any attempt to use [WR] types statistics to study the populations of the central stars and their evolution.

4.5. Do [WR] PNe occur more frequently in the Galactic bulge than in the disk?

We now compare the global characteristics of the [WR] PNe in our "merged sample" with those of the remaining PNe in this sample. Figure 1 shows that the [WR] PNe are more concentrated than the non [WR] PNe in the (l_{II}, b_{II}) diagram and have also larger Hβ fluxes. It is interesting that the [WR] PNe that lie close to the center of the Galaxy are of late [WC11] type.

Among the objects whose spectra we examined, there are 15 [WR] PNe among a total of 94 objects in the *b* subsample and 3 [WR] PNe among a total of 52 objects in the *d* subsample. Thus [WR] PNe appear preferentially in the bulge population than in the disk population, at least in the direction of the Galactic bulge. Does this mean that the *real* proportion of [WR] PNe is larger in the former than in the latter? Since *all* the spectra from our "merged sample" have been obtained in the same conditions and have been examined in a similar way for the possible presence of [WR] stars, the only effect to consider is whether it is easier to recognize a [WR] star in bulge or in disk PNe. A priori, it is easier to recognize a [WR] in a nebula of large angular dimensions and relatively close-by. Therefore, we conclude that the true proportion of [WR] PNe is significantly larger in the bulge than in the disk. Keeping in mind the considerations in Sect. 4.4, this could indicate that, in the direction of the Galactic bulge, the central star masses are likely smaller, on average, in the bulge than in the disk.

5. Abundances

5.1. Oxygen abundances: Bulge versus disk

Cuisinier et al. (2000) compared the oxygen abundances of bulge and disk PNe (their Fig. 5) by considering their own sample for the bulge (which indeed strictly obeys our criteria for sample *b*) with data taken from Maciel & Köppen (1994) for the Galactic disk. They found that the oxygen abundances in bulge PNe are comparable to those in disk PNe, with a slightly higher proportion of high abundances in the bulge. However, the distributions of the oxygen abundances in PNe in the entire Galactic disk shows important gradients (Maciel & Köppen 1994; Maciel & Quireza 1999) so that such a comparison is of limited utility. With our merged data set, we can do somewhat better, because our sample *d* contains only objects in the direction of the Galactic bulge, and is likely dominated by objects located between the Sun and the Galactic center, with a larger proportion of objects at small galactocentric distances.

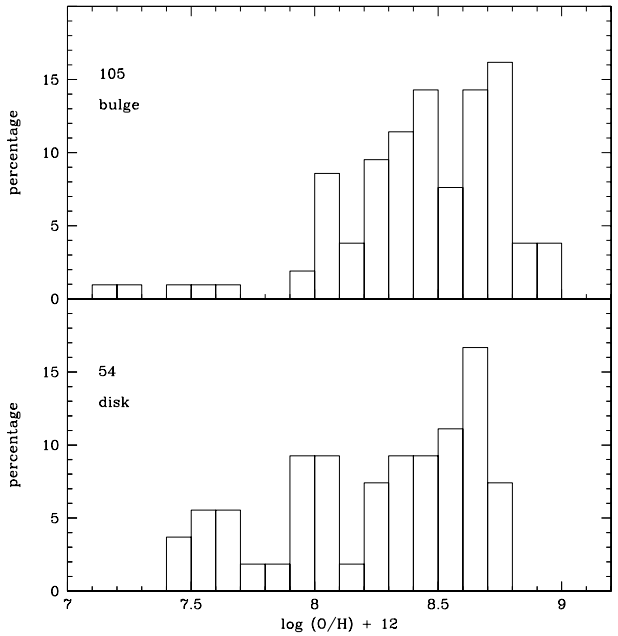

Fig. 11. The histogram of the oxygen abundances we derived for the objects of our merged sample that pertain to the bulge subsample *b* (*top panel*) and for the objects that pertain to the disk subsample *d* (*bottom panel*) as defined in Sect. 2.2.

In Fig. 11, we show the histograms of the oxygen abundances for our sample *b* and *d*. One can see that the distribution is significantly narrower and more skewed to high O/H values in sample *b*. Non parametric statistical tests confirm this impression. The median value, and the 25 and 75 percentiles are 8.45 (8.21, 8.68) for sample *b* while they are 8.32 (7.93, 8.59) for sample *d*. The above considerations concern the nominal abundances derived from the observed line intensities. Errors in abundance derivations were discussed in Sect. 3.2. They are not expected to change our conclusions, except perhaps as regards the PNe which were found to have very low abundances. However, of the 5 PNe with a nominal value of log O/H + 12 smaller than 7.5 in the entire sample, 2 have abundance with better than 0.2 dex accuracy as seen in Fig. 4, and for the three remaining ones, two pertain to sample *b* and one in sample *d*. In addition, we should consider that, within our entire sample of observations, there are 4 objects in sample *b* and 1 in sample *d* for which the abundances could not be derived because the electron temperature is unknown. The relative proportion of *b* and *d* objects among these 4 objects, compared to a total of 105 objects in sample *b* and 54 objects in sample *d* implies that our conclusions are not likely to be affected by errors in the abundances. Clearly, better data on a larger sample would be needed to confirm this.

From the compilation of Maciel & Quireza (1999), which concerns PNe at Galactocentric distances between 3 and 14 kpc, the oxygen abundance steadily increases inwards, reaching log O/H +12 of about 8.7 at the Galactocentric distance of the Sun and about 9 at 3 kpc, with a dispersion of

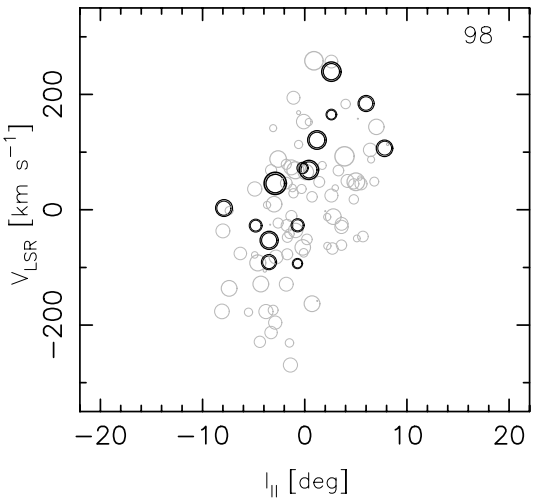

Fig. 12. The (V_{lsr}, l_{II}) diagram for samples *b* only. The radius of the circle is proportional to O/H.

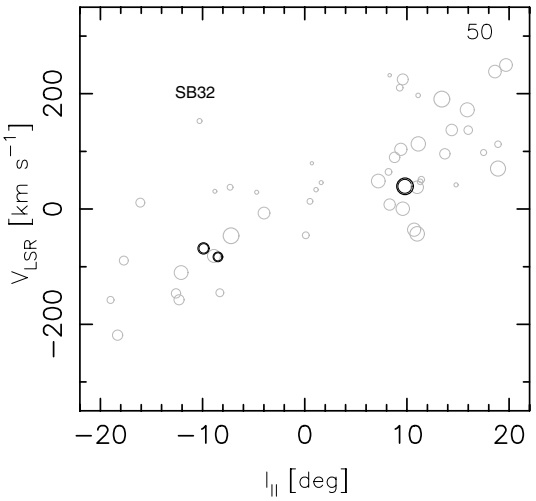

Fig. 13. The (V_{lsr}, l_{II}) diagram for samples *d* only. The radius of the circle is proportional to O/H. The object SB 32 (PN G 349.7-09.1), which possibly belongs to the halo (see Sect. 5.1) has been labelled.

about ±.2 dex. Comparing these values with the histogram shown in Fig. 11 for our *d* sample (lower panel), we conclude that O/H levels off and probably even decreases in the most internal parts of the Galactic disk. This is well in line with the findings of Smartt et al. (2001) based on abundance determination of four B-type stars.

As concerns the bulge, the oxygen abundance distribution we find has roughly the same shape as that found by Zoccali et al. (2003) for the metallicity distribution of bulge giants (with a sharp cut-off at the high abundance end and a long tail towards low abundances), but it is narrower by roughly 0.3 dex.

It is remarkable also that the median oxygen abundance in sample *b* is larger by about 0.2 dex than that of our sample *d*.

We also examined whether oxygen abundances show any trend with some other properties. The most interesting results are seen in Figs. 12 and 13, where we show again the (V_{lsr}, l_{II}) diagram for samples *b* and *d* separately, this time representing the nebulae by circles whose surface is

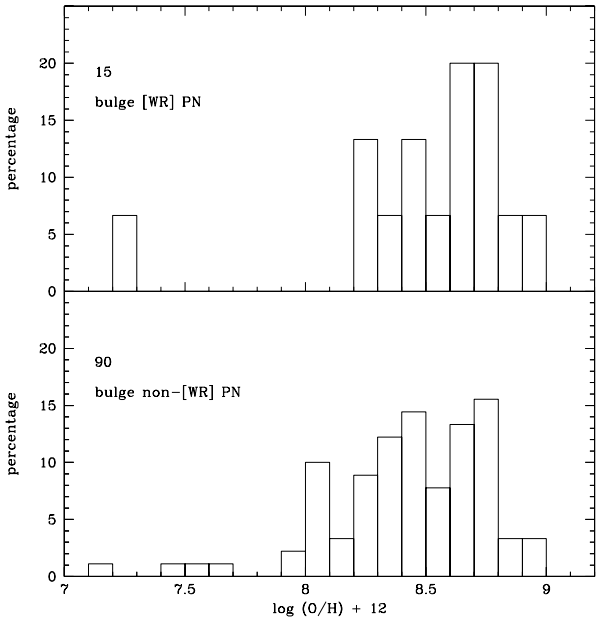

Fig. 14. The histogram of the oxygen abundances we derived for the [WR] PNe of our merged sample (*top panel*) and for the non-[WR] PNe (*bottom panel*) that pertain to the bulge subsample *b* as defined in Sect. 2.2.

proportional to O/H. Figure 13 displays one important feature. While most of the objects are roughly consistent with rotation of the Galactic disk, one object is clearly an outlier. This is SB 32 (PN G 349.7-09.1), which has log O/H + 12 = 7.77 (+0.47, −0.24). Both its position in the (V_{lsr}, l_{II}) diagram and its low oxygen abundance indicate that this PN likely belongs to the Galactic halo and not to the disk.

In Fig. 12, which concerns sample *b*, we may note that the PNe with smaller oxygen abundances tend to have smaller radial velocities.

5.2. Oxygen abundances: [WR] PNe versus other PNe in the bulge

When comparing the abundances of [WR] PNe and non[WR] PNe, Górny & Stasińska (1995) refrained from comparing oxygen abundances, which are strongly affected by the location of the PN in the Galaxy. With our present work, we are in a much more favourable situation. We have a sample of PNe in the bulge out of which was drawn a sample of [WR] PNe. Figure 14 shows in the top panel the histogram of the oxygen abundances for the [WR] PNe in our sample *b* while in the bottom panel the same is shown for the remaining PNe in this sample. Although the sample of [WR] PNe is small (15 objects), the distributions are remarkably similar and undistinguishable by non parametric statistical tests.

We thus conclude that the oxygen abundances in [WR] stars are not significantly affected by nucleosynthesis and mixing in the progenitors. This implies that [WR] PNe, similarly to ordinary PNe, can be used to determine the oxygen abundance of the media out of which the progenitors were born.

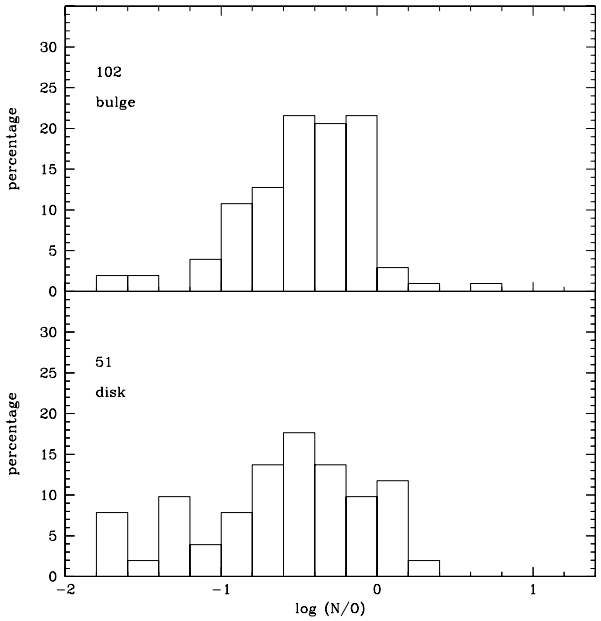

Fig. 15. The histogram of the N/O ratios we derived for the PNe of our merged sample that pertain to the bulge subsample *b* (*top panel*) and for the PNe that pertain to the disk subsample *d* (*bottom panel*) as defined in Sect. 2.2.

6. N/O ratios

Figure 15 show the histograms of the N/O ratios in samples *b* (top panel) and *d* (bottom panel) respectively. The distributions are seen to be similar and they are undistinguishable by non parametric statistical tests.

Figure 16 shows the histogram of N/O in the [WR] PNe of sample *b*. Although also in this case the number of objects is small (15), again we can conclude that the distribution is indistinguishable, statistically, from the previous ones.

We thus conclude that, although N is known to be produced and dredged-up by the PNe progenitors, and that the nitrogen enrichment is expected to by a function of the progenitor's mass and of the mass loss rate (Marigo 2001), a statistical study such as the one we present is not able to give any real clue.

7. Conclusions

We have conducted a statistical analysis of planetary nebulae in the direction of the Galactic bulge, with the double aim of a better understanding of the global properties of PNe with Wolf-Rayet type central stars, and of a more refined characterization of the different populations of PNe that are seen in this direction.

We have performed new observations of 44 PNe in the direction of the Galactic bulge, and merged them with data from previous studies suitable for our purposes, constituting a sample of 164 PNe.

We have distinguished, in this merged sample, the PNe most probably pertaining physically to the Galactic bulge, and the PNe most likely belonging to the Galactic disk.

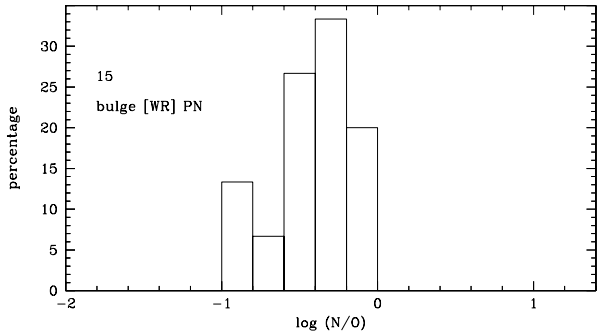

Fig. 16. The histogram of N/O ratios derived for the [WR] PNe of our merged sample that pertain to the bulge subsample *b* as defined in Sect. 2.2.

We have determined the chemical composition of all the 164 objects in a coherent way and discussed the uncertainties in the derived abundances.

We have looked for stellar emission features in all the 164 objects. This search resulted in the discovery of 14 new [WR] stars and 15 new weak emission line central stars, significantly enlarging the number of emission line stars known in the direction of the Galactic bulge. We have also performed a spectral classification of all the new [WR] stars.

Our findings were then discussed with the aim of getting some clues on [WR]PN production and evolution, on the various populations of planetary nebulae seen in the direction of the Galactic disk, and on the distribution of oxygen abundance in the Galaxy as measured by planetary nebulae. Particular attention was paid to take into account selection effects.

Our main results are the following:

We confirm that the spectral type distribution of [WR] stars is very different in the bulge and in the disk of the Galaxy. However, we show that the selection effects, being not the same between bulge and disk PNe, can explain, at least in part, this observed difference in spectral type distribution.

We show that the proportion of [WR] PNe with respect to the remaining PNe is significantly larger in the bulge than in the disk. We show that this is likely an indirect indication that the central star masses are, on average, smaller in the bulge than in the disk.

There is no difference, in the Galactic bulge, between the oxygen abundances in [WR] PNe and in the remaining PNe. This implies that the oxygen abundances in [WR] stars are not significantly affected by nucleosynthesis and mixing in the progenitors. This is the first time that such an inference can be made, since this is the first time that a significant sample of [WR] PNe and non-[WR] PNe belonging exactly to the same Galactic population is available.

The O/H gradient of the PNe population in the Galactic disk flattens in the most internal parts of the Galaxy and possibly changes sign, in line with results from abundance determinations in B-type stars (Smartt et al. 2001).

The median oxygen abundance in the bulge is larger by 0.2 dex than that PNe seen in the direction of the bulge but pertaining to the disk.

The oxygen abundance distribution for the bulge PNe has a shape similar to that found by Zoccali et al. (2003) for the

metallicity distribution of bulge giants (with a sharp cut-off at high abundance and a long tail at low abundance), but it is narrower by about 0.3 dex.

The bulge PNe with smaller oxygen abundances tend to have smaller radial velocities.

Among the PNe seen in the direction of the bulge and pertaining to our merged sample, SB 32 (PN G 349.7-09.1) has a location in the ($V_{\rm lsr}$, $l_{\rm II}$) diagram and a low oxygen abundance, indicating that it probably belongs to the Galactic halo population.

Finally, the distributions of N/O are the same in the disk PNe seen in the direction of the bulge and in PNe pertaining physically to the bulge. They are also the same in [WR] PNe and non[WR] PNe pertaining to the bulge.

Some of these findings are in line with what was known before. Others are rather unexpected. Taken together, and combined with data from other sources, they should provide interesting constraints on the stellar populations in the inner parts of the Galaxy, on the Galaxy chemical evolution and on the causes of the [WR] phenomenon.

Acknowledgements. S.K.G. acknowledges the "Jumelage Astronomie France-Pologne" as well as the Polish grant KBN 2.PO3D.017.25 for financial support. G.S. acknowledges the "Jumelage Astronomie France-Pologne" and the "PICs Franco-Bresilien" for financial support. A.V.E. acknowledges FAPESP for his graduate fellowship.

References

Acker, A., & Neiner, C. 2003, A&A, 403, 659
Acker A., Ochsenbein F., Stenholm B., et al. 1992, Strasbourg-ESO Catalogue of Galactic Planetary Nebulae. ESO publication
Acker, A., Górny, S. K., & Cuisinier, F. 1996, A&A, 305, 944
Beaulieu, S. F., Dopita, M. A., & Freeman, K. C. 1999, ApJ, 515, 610
Beaulieu, S. F., Freeman, K. C., Kalnajs, A. J., et al. 2000, AJ, 120, 855
Blöcker, T. 1995, A&A, 299, 755
Blöcker, T. 2001, Ap&SS, 275, 1
Blöcker, T., Osterbart, R., Weigelt, G., et al. 2001, in Post-AGB objects as a phase of stellar evolution, ed. R. Szczerba, & S. K. Górny, Astrophysics & Space Science Library (Kluwer), 241
Chiappini, C., Matteucci, F., & Romano, D. 2001, ApJ, 554, 1044
Crowther, P. A., De Marco, O., & Barlow, M. J. 1998, MNRAS, 296, 367
Cuisinier, F., Maciel, W. J., Köppen, J., et al. 2000, A&A, 353, 543
de Araújo, F. X., Marcolino, W. L. F., Pereira, C. B., & Cuisinier, F. 2002, AJ, 124, 464
De Marco, O. 2003, in Planetary Nebulae: their Evolution and Role in the Universe, ed. S. Kwok, M. Dopita, & R. Sutherland, ASP/IAU Publications, Proc. IAU, 209, 215
De Marco, O., & Soker, N. 2002, PASP, 114, 602
Durand, S., Acker, A., & Zijlstra, A. 1998, A&AS, 132, 13
Escudero, A. V., & Costa, R. D. D. 2001, A&A, 380, 300
Escudero, A. V., Costa, R. D. D., & Maciel, W. J. 2004, A&A, 414, 211
Górny, S. K. 2001, in Low mass Wolf-Rayet Stars: origin and evolution, ed. E. Waters, A. Zijlstra, & T. Blöcker, Ap&SS, 275, 67
Górny, S. K., & Stasińska, G. 1995, A&A, 284, 949
Górny, S. K., & Tylenda, R. 2000, A&A, 362, 1008
Górny, S. K., Stasińska, G., Szczerba, R., & Tylenda, R. 2001, A&A, 377, 1007
Herwig, F. 2001, Ap&SS, 275, 15
Hu, J. Y., & Bibo, E. A. 1990, A&A, 234, 435
Iben, I., Kaler, J. B., Truran, J. W., & Renzini, A. 1983, ApJ, 264, 605
Keenan, F. P., Aller, L. H., Bell, K. L., et al. 1996, MNRAS, 281, 1073
Koesterke, L., & Hamann, W.-R. 1997, in Planetary Nebulae, ed. H. J. Habing, & H. J. G. L. M. Lamers (Kluwer), Proc. IAU Symp., 180, 114
Kohoutek, L. 1994, Astron. Nachr., 315, 235
Leuenhagen, U., & Hamann, W.-R. 1998, A&A, 330, 265
Leuenhagen, U., Hamann, W.-R., & Jeffery, C. S. 1996, A&A, 312, 167
Liu, X.-W. 2002, Rev. Mex. A&A (Serie de Conferencias), 12, 70
Maciel, W., & Köppen, J. 1994, A&A, 282, 436
Maciel, W., & Quireza, C. 1999, A&A, 345, 629
Marigo, P. 2001, A&A, 370, 194
Méndez, R. H., & Niemela, V. S. 1982, in Wolf-Rayet Stars, ed. de Loore & Willis, IAU Symp., 99, 457
Parker, Q. A., & Morgan, D. H. 2003, MNRAS, 341, 961
Parker, Q. A., Phillipps, S., & Morgan, D. H. 1999, in New Perspectives on the Interstellar Medium, ed. Taylor, Landecker, & Joncas, ASP Conf. Ser., 168, 126
Parker, Q. A., Hartley, M., Russeil, D., et al. 2003, in Planetary Nebulae: their Evolution and Role in the Universe, ed. S. Kwok, M. Dopita, & R. Sutherland, ASP/IAU Publications, IAU Symp., 209, 25
Peña, M., Hamann, W.-R., Koesterke, L., et al. 1997, ApJ, 491, 233
Peña, M., Stasińska, G., & Medina, S. 2001, A&A, 367, 983
Seaton, M. J. 1979, MNRAS, 187, 73
Smartt, S. J., Venn, K. A., Dufton, P. L., et al. 2001, A&A, 367, 86
Stasińska, G., & Tylenda, R. 1994, A&A, 289, 225
Stasińska, G., Tylenda, R., Acker, A., & Stenholm, B. 1991, A&A, 247, 173
Stasińska, G., Tylenda, R., Acker, A., & Stenholm, B. 1992, A&A, 266, 486
Stasińska, G., Richer, M. G., & McCall, M. L. 1998, A&A, 336, 667
Szczerba, R., Górny, S. K., Stasińska, G., et al. 2001, in Low mass Wolf-Rayet Stars: origin and evolution, ed. E. Waters, A. Zijlstra, & T. Blöcker, Ap&SS, 275, 113
Szczerba, R., Volk, K., & Górny, S. K. 2003, in Planetary Nebulae: their Evolution and Role in the Universe, ed. S. Kwok, M. Dopita, & R. Sutherland, ASP/IAU Publications, IAU Symp., 209, 301
Tylenda, R. 1996, in Hydrogen-Deficient Stars, ed. C. S. Jeffery, & U. Heber, ASP Conf. Ser., 101
Tylenda, R., Acker, A., Stenholm, B., et al. 1991, A&AS, 89, 77
Tylenda, R., Acker, A., & Stenholm, B. 1993, A&AS, 102, 595
Tylenda, R., Stasińska, G., Acker, A., & Stenholm, B. 1994, A&AS, 106, 559
van der Hucht, K. A., Conti, P. S., Lundström, I., & Stenholm, B. 1981, Space Sci. Rev., 28, 227
Zijlstra, A. A., Acker, A., & Walsh, J. R. 1997, A&AS, 125, 289
Zoccali, M., Renzini, A., Ortolani, S., et al. 2003, A&A, 399, 931